PAPER • OPEN ACCESS

Magnetic turbulence and long-range correlation studies in the GOLEM tokamak

To cite this article: G Sarancha *et al* 2021 *J. Phys.: Conf. Ser.* **2055** 012003

View the article online for updates and enhancements.

Magnetic turbulence and long-range correlation studies in the GOLEM tokamak

G Sarancha[1,2,5]**, V Svoboda**[3]**, J Stockel**[3] **and A Melnikov**[1,2,4]

[1] National Research Centre "Kurchatov Institute", Moscow, 123182 Russia
[2] National Research University "Moscow Institute of Physics and Technology", Dolgoprudny, 141700 Russia
[3] Czech Technical University in Prague, Prague, 16 00 Czech Republic
[4] National Research Nuclear University "Moscow Engineering Physics Institute", Moscow, 115409 Russia

[5] E-mail: sarancha.ga@phystech.edu

Abstract. The small university-scale tokamak GOLEM equipped with the electric and magnetic probes becomes a test bench for studying the plasma turbulence and Zonal Flows, which are the essential processes affecting the plasma confinement. The broadband ($f_{BB} <$ 250 kHz) magnetic turbulence was detected for the first time using the Mirnov probes. The two-dimensional (frequency–wavelength) Fourier power spectra $S(k, f)$ of the magnetic turbulence indicate the turbulence poloidal propagation. The long-range correlations (LRC) between the signals of magnetic and electric probes installed at different toroidal cross-sections were detected in the low-frequency range ($f_{LRC} < 60$ kHz), which is similar to the plasma potential LRC range observed in other devices.

1. Introduction

To expand the experimental database on plasma turbulence and confinement properties, it will be helpful to investigate the operation ranges of plasma parameters, within which these phenomena are observed at different machines: from the large machines to the small-scale ones with the low electron temperature and plasma density corresponding to the edge plasmas of the larger machines. From this point of view, the small and medium-size fusion devices could be very helpful for the mainstream plasma research in this field [1, 2].

The present study is focused on the electrostatic and magnetic turbulence and their correlation properties in the GOLEM tokamak. The long-range correlations are the characteristic features of the Zonal Flows, which are the mechanism for the broadband turbulence self-regulation [3]. Recently, the Zonal Flows and Geodesic Acoustic Modes, which are their higher frequency counterparts, have been actively studied in tokamaks [4, 5, 6, 7] and stellarators [8, 9, 10, 11] of the small and medium size. Searching and studying the Zonal Flows could be one of the most important contributions of the GOLEM tokamak to the mainstream fusion researches.

2. Setup and diagnostic of the GOLEM tokamak

The ohmic heated tokamak GOLEM ($R = 0.4$ m, $a = 0.085$ m, $B_t < 0.4$ T, $I_{pl} < 10$ kA) operates with hydrogen, helium and argon plasmas at the Czech Technical University in Prague [1, 12]. In the typical plasma discharge, the line-averaged density is up to $\bar{n}_e \sim 1 \times 10^{19}$ m^{-3}, and the central electron

temperature is $T_e \sim 100$ eV. The GOLEM has the molybdenum poloidal limiter and stainless steel chamber surrounded by the copper shell providing the passive stabilization of the plasma column.

The virtual control room provides the remote control of the GOLEM operation [13]. The probe diagnostics consists of the four Mirnov coils (MC-in, MC-out, MC-up, MC-down) and the Langmuir probe (LP), the arrangement of which is presented in Fig. 1a and 1b.
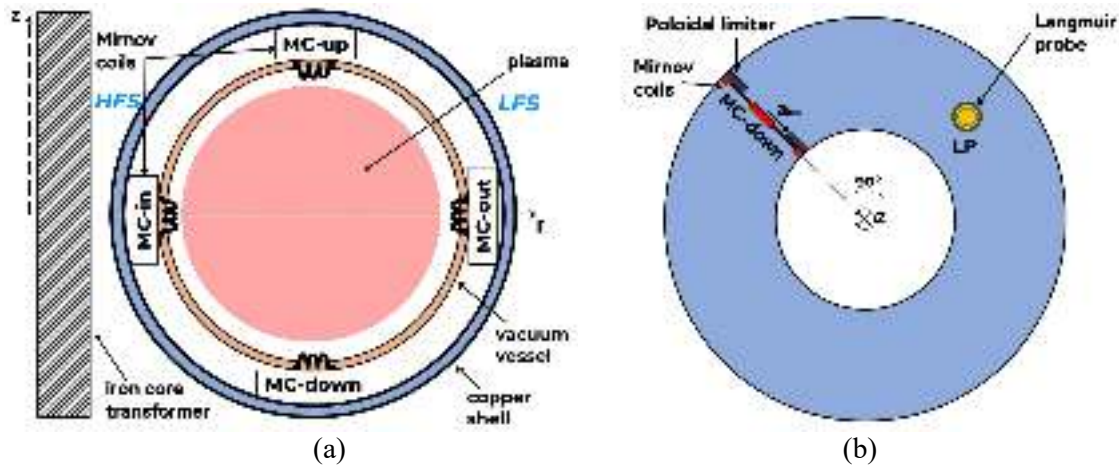

(a)   (b)

Figure 1. Arrangement of the GOLEM probe diagnostics (a) side view, (b) bottom view. Mirnov coils are installed behind the circular limiter, $a_{lim} = 0.085$ m. The Langmuir probe is shifted toroidally with respect to the Mirnov probes by 90°.

Plasma position inside the vacuum chamber is determined by measuring the relative changes in the Mirnov coil signals and calculated in accordance with Eqs. 1 and 2:

$$\Delta z = \frac{B_{MC-} - B_{MC-down}}{B_{MC-up} + B_{MC-}} \tag{1}$$

$$\Delta r = \frac{B_{MC-ou} - B_{MC-in}}{B_{MC-ou} + B_{MC-in}} \tag{2}$$

where Δz and Δr are the vertical and horizontal displacements with respect to the center of the vacuum chamber.

3. Experimental results

During the experiment, the maximum plasma current $I_{pl\,max}$, the average plasma density $\bar{n}_e$, and the type of working gas (hydrogen H_2 or helium He) were varied from shot to shot. Typical plasma scenarios for hydrogen and helium discharges are shown in Fig. 2a and 2b, respectively. In these figures, black curves indicate the loop voltage U_{loop}, blue and red lines correspond to the toroidal magnetic field B_t and plasma current I_{pl} measured by the Rogowski coil, respectively. Red dashed line corresponds to the maximal plasma current. Discharge starts simultaneously with plasma current pulse and ends with plasma current quench (rapid drop), time T_{dis} is defined as discharge duration, and the voltage U_{BD} corresponds to loop voltage breakdown. The discharges in helium are characterized by the higher loop voltage and smaller plasma current as compared to the discharges in hydrogen. During the discharge in hydrogen, the plasma current oscillations occur when the maximum plasma current $I_{pl\,max}$ is reached. And during the discharge in helium, the plasma current smoothly decreases without any instabilities.
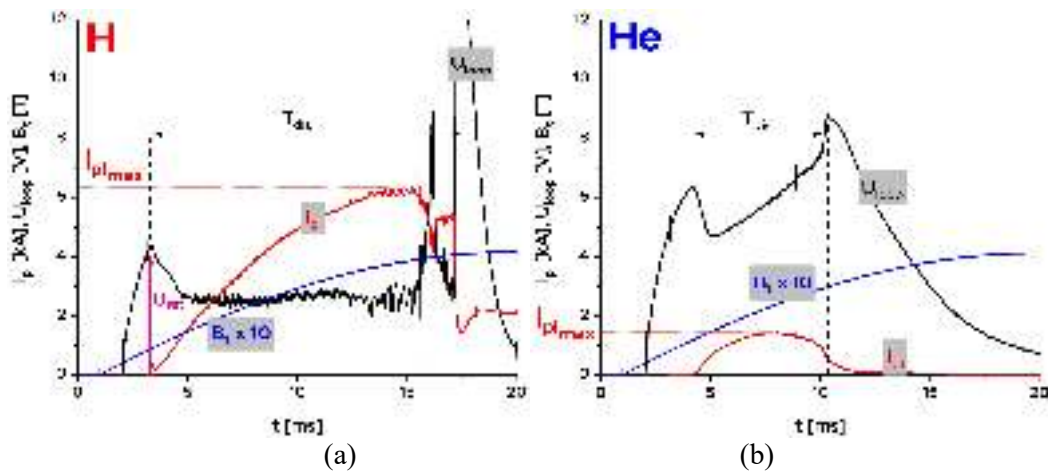
Figure 2. Discharge scenarios for (a) hydrogen and (b) helium plasmas.

For the moment, there are no means for fixing the plasma column position with respect to the vacuum chamber walls, and it changes during the discharge. The displacements of hydrogen and helium plasmas at different currents $I_{pl\ max}$ are shown in Fig. 3. It can be seen that they are displaced in different directions. For hydrogen and helium plasmas, working domains of plasma displacements at time of the maximum plasma current are also indicated in Fig. 3. Each plasma shot is presented by two points: stars and circles correspond to the vertical and horizontal displacements (as shown by two double-headed arrows). Figure also demonstrates that in the vacuum chamber, the helium plasma moves upward ($\Delta z > 0$) and inward ($\Delta r < 0$), that is, to the High Field Side. Points show the plasma position averaged over 20 μs in the vicinity of time, when the plasma current reaches its maximum $I_{pl\ max}$.
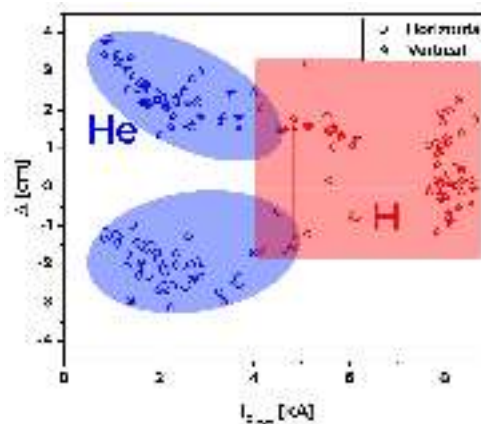

Figure 3. Vertical Δz and horizontal Δr displacements of the plasma column for hydrogen (red) and helium (blue) plasmas. As an example, vertical arrows denote the points corresponding to the same shot.

3.1. Broadband magnetic turbulence

Fig. 4a shows the two-dimensional Fourier spectrum $S(k, f)$ of the magnetic fluctuations recorded by the probes MC-out and MC-down. The Fourier spectrum was obtained using the two-point correlation technique [14]. The figure gives a pattern of the broadband magnetic turbulence, which shows that there is the systematic linear correlation between the cross-phase (wave vector k) and the oscillation frequency f indicating the poloidal turbulence rotation from the bottom to the Low Field Side. Fig. 4b shows the time evolution of the cross-phase between the signals of the MC-out and MC-down probes. It can be seen that the cross-phase linearly increases from zero to π, as the frequency f varied from 0 to approximately 150 kHz, and then it changes the sign to $-\pi$ and further increases up to 250 kHz.

The fact that for the blue curve, the frequency, at which the cross-phase reaches π, exceeds that for the red curve indicates an increase in the rotational velocity.
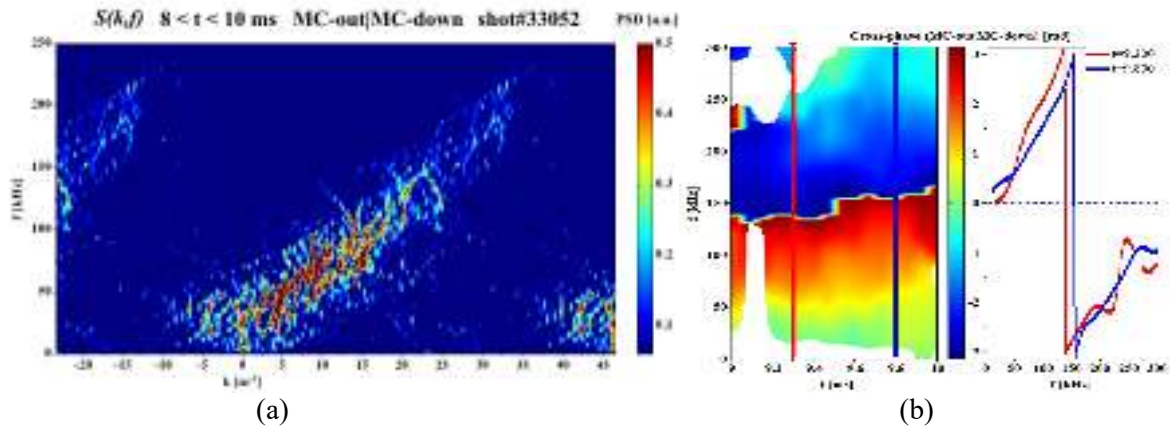

(a)   (b)

Figure 4. (a) Two-dimensional spectrum of magnetic fluctuations $S(k, f)$ averaged over 2 ms ($8 < t < 10$ ms) and (b) time evolution of the cross-phase of two MC signals (left). Only statistically significant values are presented (quadratic coherence coefficient is >0.2); and (right) cross-phase as a function of frequency for two times marked in the left figure.

3.2. Long-range electromagnetic correlations

The Long-Range Correlations (LRC) is a tool for studying the global modes of plasma oscillations such as the Geodesic Acoustic Modes and Zonal Flows. At the GOLEM tokamak, the electric and magnetic probes are shifted in the toroidal direction by 90°, as shown in Fig. 1b, so the correlations between the probe signals could be found. The coefficients of coherence and cross-phases between the magnetic oscillations measured by the Mirnov coils and the floating potential oscillations measured by the Langmuir probe are shown in Fig. 5. One can see there is the dominant mode with a frequency of approximately 20–60 kHz in the hydrogen plasma, which is more pronounced in the magnetic signal. This mode is observed in the developed discharge stage, when the plasma current I_{pl} is close to its maximum $I_{pl\ max}$, but the quenching instabilities are still not developing. In the frequency range of this mode, high coherence was observed between the signals of the Langmuir probe and magnetic probes. The quadratic coherence coefficient and cross-phase between the signals of the magnetic and Langmuir probes averaged over 4 ms (from 8 to 12 ms) are shown in Fig. 5b.
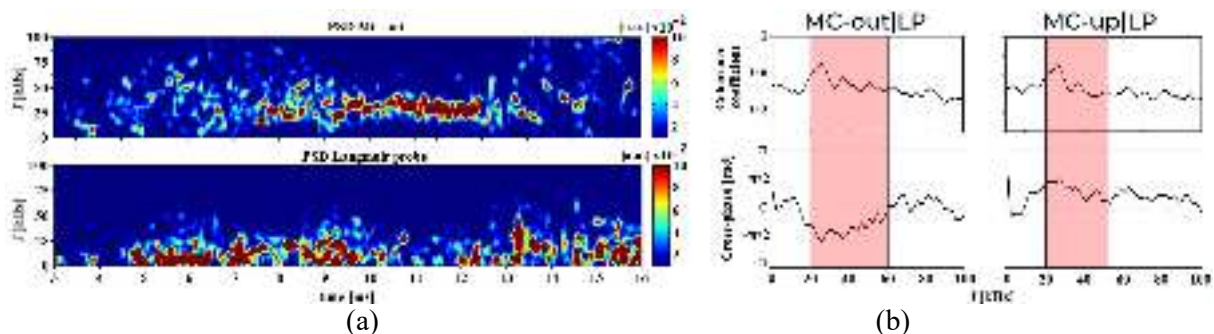

(a)   (b)

Figure 5. (a) Power spectral density of the signals of the MC-out (top) and Langmuir (bottom) probes and (b) quadratic coherence coefficient (top) and cross-phase between the signals of the magnetic and Langmuir probes (bottom).

4. Summary

The first observations of the long-range electromagnetic correlations and broadband magnetic turbulence observed in plasma of the GOLEM tokamak are presented. It is found that the development of the broadband (up to 250 kHz) magnetic turbulence is noticeable only in the helium plasma.

In the hydrogen plasma, the long-range correlations (f = 20–60 kHz, coefficient of coherence is up to 0.6) were observed between the signals of the electric and magnetic probes spaced by a distance of more than 60 cm.

The studies of such oscillations are important for understanding the mechanism for self-organization of the broadband turbulence and its development at the larger-scale devices.

Acknowledgments

References

[1]   Gryaznevich M et al. 2009 *Nucl. Fusion* **49** 104026
[2]   Van Oost G et al. 2003 *Plasma Phys. Control. Fusion* **45** 621
[3]   Fujisawa A et al. 2007 *Nucl. Fusion* **47** S718
[4]   Melnikov A et al. 2005 *Czech. J. Phys.* **55** 349
[5]   Melnikov A *et al* 2015 *J. Phys.: Conf. Ser.* **591** 012003
[6]   Melnikov A et al. 2006 *Plasma Phys. Control. Fusion* **48** S87
[7]   Basu D et al. 2018 *Nucl. Fusion* **58** 024001
[8]   Fujisawa A et al. 2004 *Phys. Rev. Lett*. **93** 65002
[9]   Alonso J et al. 2017 *Phys. Rev. Lett*. **118** 185002
[10]   Melnikov A et al. 2017 *Nucl. Fusion* **57** 072004
[11]   Melnikov A et al. 2018 *Plasma Phys. Control. Fusion* **60** 084008
[12]   Gryaznevich M et al. 2020 *Plasma Sci. Technol*. **22** 055102
[13]   Svoboda V et al. 2019 *Journal of Fusion Energy* **38** 253
[14]   Eliseev L et al. 2012 *Plasma and Fusion Research* **7** 2402064